



Observation of a fifth order optical nonlinearity in 29 kDa Au@alkanethiol clusters excited in the visible

Jinto Thomas ^a, M. Anija ^a, Jobin Cyriac ^b, T. Pradeep ^{b,*}, Reji Philip ^{a,*}

^a Optics Group, Raman Research Institute, C.V. Raman Avenue, Sadashivanagar, Bangalore 560080, India

^b Department of Chemistry and Sophisticated Analytical Instrument Facility, Indian Institute of Technology Madras, Chennai 600 036, India

Received 1 January 2005

Abstract

The absorptive optical nonlinearity in nanoclusters of Au@hexanethiol and Au@dodecanethiol has been investigated. From the mass spectra, each cluster is estimated to contain about 140 atoms of gold. The optical absorption spectra of the clusters show a gradual increase in absorbance towards the UV region, over which an extremely weak surface plasmon resonance (SPR) is superposed. No plasmon bleach effects are seen when the samples are excited with nanosecond laser pulses at 532 nm. Instead, a reduced transmission behavior is observed, which fits to a three-photon absorption mechanism. We propose that this nonlinearity is caused by two-photon induced excited state absorption occurring in the nanoclusters. Femtosecond pump–probe studies show that when excited and probed at 400 nm, the nonlinearity is very fast with a lifetime of less than 2 ps.

© 2005 Elsevier B.V. All rights reserved.

1. Introduction

Optical properties of metal nanoparticles is an active area of current research, owing to their importance in photonics and nanotechnology. A number of pioneering studies have appeared on their excited state dynamics [1–5]. Measurements on ligand-protected and oxide-protected metal nanoclusters have shown that they are very good optical limiters. From earlier studies we had found that at high laser fluences thermally induced scattering results in optical limiting [6], while at high intensities free carrier absorption had a contribution [7].

An important deciding factor in the sign of the nonlinearity of metal nanoclusters is the surface plasmon resonance (SPR), which leads to saturable absorption-like behavior upon laser excitation [8]. For Au, the SPR band is typically centered around 530 nm. It was seen earlier that SPR saturation could partially offset

the limiting mechanisms in relatively larger (>2 nm) nanoclusters [6,7]. Therefore in the present work, we have investigated the nonlinear transmission in smaller nanoclusters of Au@hexanethiol and Au@dodecanethiol, having particle sizes in the range of 1 nm. The SPR band is substantially suppressed in these clusters, so that the optical absorption spectra show only a very weak structure around the SPR wavelength. Using 7 ns laser pulses at 532 nm, an exclusive optical limiting behavior has been observed, without any indications of an SPR bleach. The temporal dynamics of the nonlinearity also is studied using pump–probe measurements at 400 nm.

2. Experimental

2.1. Synthesis and characterization

The synthesis of the clusters was carried out under ambient conditions by the Brust method [9], using

* Corresponding authors. Fax: +91 80 2361 0492.

E-mail addresses: pradeep@iitm.ac.in (T. Pradeep), reji@rri.res.in (R. Philip).

hexanethiol and dodecanethiol as protecting species. Details of the synthesis are given elsewhere [10]. In short, 20 ml of 50 mM aqueous HAuCl_4 solution and 80 ml (4 mM) tetra-*n*-octylammonium bromide (TOAB) in toluene were mixed and stirred vigorously. Then a 3 mM solution of the respective thiol (hexanethiol or dodecanethiol) in toluene was added and the resulting mixture was stirred for an additional 20 min. Aqueous 10 mM sodium borohydride (10 ml) was introduced at once to the stirring mixture. The desired product was obtained after vigorous stirring for 12 h (hexanethiol) and 2 days (dodecanethiol), respectively. The precipitate was filtered, redissolved in toluene and reprecipitated with excess propanol; the procedure was repeated twice to ensure that the excess disulfide/thiol was removed. At this stage, we adopted column chromatographic techniques for the separation of the required mass range. This precipitate was loaded onto silica column (60–120 mesh) and eluted by 5% ethyl acetate/hexane mixture. The eluted fractions were evaporated and the materials were collected as dry powders. The mass of the cluster of interest was confirmed to be 29 kDa by its matrix assisted laser desorption ionization (MALDI – Voyager DE-PRO Biospectrometry Workstation from Applied Biosystems) mass spectrum. When the near-absence of the SPR band in the UV/Vis spectrum (Perkin–Elmer Lambda 25 UV/Vis spectrometer) also is considered, it can be concluded that the present sample contains 29 kDa cluster compound exclusively. The MALDI mass and optical absorption spectra are given in Fig. 1. Similar MALDI mass and UV/Vis results have been obtained for the 29 kDa-optimized preparations of Au@dodecanethiol using the same synthetic procedure.

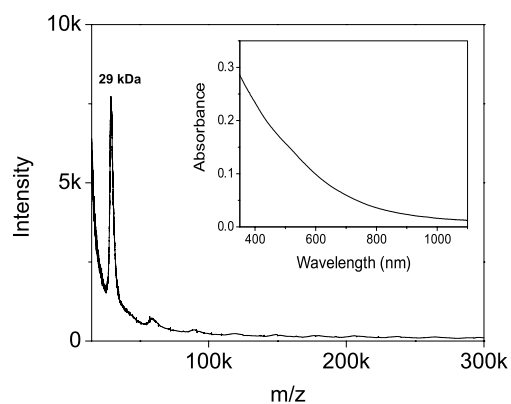


Fig. 1. MALDI-TOF spectrum of column separated Au@hexanethiol cluster compound with the matrix, indole acrylic acid (ratio 1:5) showing the presence of 29 kDa clusters exclusively. A minor peak due to the dimer formed during the ionization process [11] is also seen. *Inset*: Optical absorbance spectrum of the same sample, showing an extremely weak surface plasmon resonance around 523 nm.

3. Experimental

The nonlinear transmission properties of the clusters dissolved in toluene were investigated at 532 nm, using 7 ns laser pulses from a frequency doubled, Q-switched Nd:YAG laser. From beam measurements using the knife-edge method, the laser was found to have a gaussian profile. The pulse repetition rate was approximately 1 Hz, and the energy reaching the sample was appropriately attenuated using neutral density filters. The intensity dependent transmission was measured using an open aperture *z*-scan [12] set-up, which was automated. In the *z*-scan, the laser beam is focused using a lens, and the sample is translated along the beam axis (*z*-axis) through the focal region over a length, several times that of the confocal distance. At each position, *z*, the sample sees a different laser fluence, and the position dependent (i.e., fluence-dependent) transmission is measured using an energy probe placed after the sample. In our experiments, we used a lens of 190 mm focal length, and the focal spot diameter was 34 μm . The pulse-to-pulse energy stability of the laser was found to be approximately $\pm 5\%$. Therefore, the energy of each pulse was measured by a calibrated reference detector, and used in the calculations, to get a better numerical fit of the experimental data to the transmission equations. To investigate the possibility of induced light scattering in the present samples, a photomultiplier tube (PMT) was used in addition to the existing detectors, to record the scattered radiation [6]. The PMT was fixed at an angle of about 15° from the beam axis. By mounting the sample and PMT on the same translation stage, it was ensured that the PMT was at the same distance from the sample throughout the scan.

To obtain the temporal evolution of the nonlinear transmission, pump–probe measurements were performed using 100 fs laser pulses taken from a frequency doubled (400 nm) Ti:Sapphire Chirped Pulse Amplifier laser (Spectra Physics, TSA-10). The pulse repetition rate was approximately 1 Hz.

4. Results and discussion

From the *z*-scan curves (Fig. 2a), we found that the nonlinearity is essentially of the reduced transmission (optical limiting) type. Limiting shown by pure toluene is negligible here, and the limiting efficiency increases substantially with sample concentration. Fig. 2b shows the PMT output (induced scattering) as a function of the input laser fluence. In general, this scattering is caused by thermally induced transient refractive index changes given by $\Delta n = (dn/dt)F_0\alpha/2\rho C_v$, where dn/dt is the thermo-optic coefficient, F_0 is the fluence, α is the absorption coefficient, ρ is the density and C_v is specific heat at constant volume. Such induced scattering contributes to optical limiting in a number of materials,

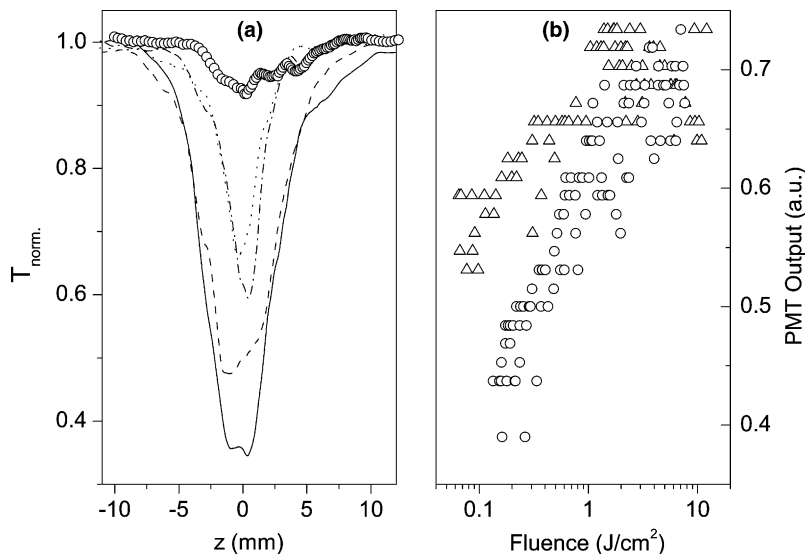


Fig. 2. (a) z -scan curves obtained for the 29 kDa Au clusters when excited with 532 nm, 7 ns pulses. The mean laser energy reaching the sample is 38 μ J. Linear transmissions are: solid curve, 0.20; dash, 0.3; dash-dot, 0.47 and dot, 0.67. Circles represent pure toluene. (b) Induced scattering signals obtained from the PMT, as a function of the input laser fluence. Linear transmissions are: circles, 0.20; triangles, 0.67.

including C_{60} [13], metal-dendrimer nanocomposites [14], and large metal clusters [6,15]. However, in the present case where the clusters are very small, induced scattering alone is insufficient to explain the observed limiting. This point is obvious from the fact that the scattering amplitudes are nearly the same irrespective of the sample concentration, particularly at higher input fluences. Therefore the observed increase in limiting with sample concentration should have a non-thermal origin. To investigate this point further, we have estimated the order of the nonlinearity from numerical fitting of the experimental data to the relevant nonlinear transmission equations [16]. It was found that the net transmission, T of the clusters could be described either by a two-photon absorption process given by,

$$T = \left((1 - R)^2 \exp(-\alpha L) / \sqrt{\pi} q_0 \right) \times \int_{-\infty}^{+\infty} \ln [1 + q_0 \exp(-t^2)] dt \quad (1)$$

or a three-photon process given by,

$$T = \left((1 - R)^2 \exp(-\alpha L) / \sqrt{\pi} p_0 \right) \times \int_{-\infty}^{+\infty} \ln \left[\sqrt{1 + p_0^2 \exp(-2t^2)} + p_0 \exp(-t^2) \right] dt, \quad (2)$$

where L and R are the sample length and surface reflectivity respectively, and α is the linear absorption coefficient. q_0 in Eq. (1) is given by $\beta(1 - R)I_0 L'_{\text{eff}}$, where β is the two photon absorption coefficient, and I_0 is the on-axis peak intensity. L'_{eff} is given by $[1 - \exp(-\alpha L)] / \alpha$. p_0 in Eq. (2) is given by $[2\gamma(1 - R)^2 I_0^2 L'_{\text{eff}}]^{1/2}$, where γ is the three photon absorption coefficient, and L'_{eff} is

given by $[1 - \exp(-2\alpha L)] / 2\alpha$. Figs. 3a,b show the least squares fits obtained for a dilute, as well as a concentrated solution, respectively. Calculated SSEs (sum of squares error) show that in the dilute solution both the above equations fit with a similar accuracy, while the three-photon fit is much better in the concentrated solution. The numerically calculated value of the three photon absorption coefficient is $2.9 \times 10^{-21} \text{ m}^3 \text{ W}^{-2}$, for the concentrated sample.

At the outset this looks curious, because in the present case, there are no compelling reasons for a pure fifth order nonlinearity to override the third order nonlinearity. However, some parallels to such behavior can be drawn from previous studies, mostly conducted in semiconductors. There, the optical nonlinearities in the transparent spectral region can be divided into two categories, namely, the third order effects arising from bound electrons, and, other effects due to the photo-generated free carriers. While third order nonlinearities are important in the femtosecond time domain, the free carrier nonlinearities become significant for nanosecond and longer pulse excitation. One consequence of this situation is that nonlinear absorption can be caused through charge carriers generated by two-photon absorption (i.e., a sequential $\chi^{(3)}:\chi^{(1)}$ effect), which will appear as a fifth order ($\chi^{(5)}$) nonlinearity [17]. Similarly, an I^5 dependence of the refractive nonlinearity also has been observed in semiconductor doped glasses, when the band gap of the semiconductor crystallites become smaller than twice the photon energy [18,19]. On the other hand, bi-photonic generation of free carriers in silver colloids was discussed by Kamat et al. [20], and the possibility of free carrier absorption contributing to the

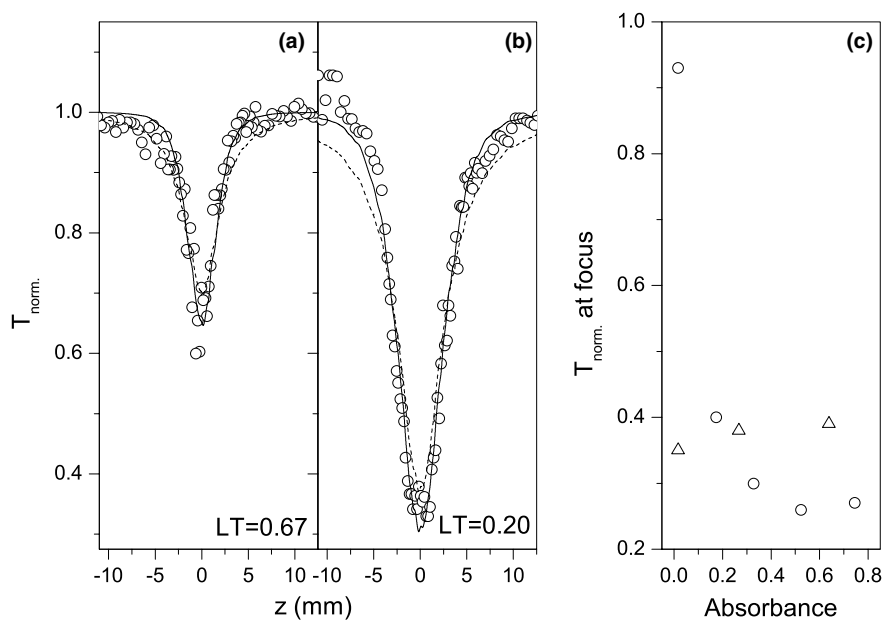


Fig. 3. (a,b) z-scan curves with numerical fits. Circles are data points. Solid curves are numerical fits to a three-photon absorption process while dotted curves are those for a two-photon absorption process. Linear transmissions are 0.67 and 0.20 as shown. The mean laser pulse energy is 38 μJ . (c) Reduction in transmission as a function of laser pulsewidth and sample concentration. Normalized transmittance of the samples at the beam focus is plotted against sample absorbance (measurements are in a 1-mm cuvette). Absorbance of pure toluene is close to zero. Triangles, 100 fs pulses (400 nm); circles, 7 ns pulses (532 nm).

nonlinearity of 3–4 nm sized clusters under picosecond excitation was suggested [7].

One way to test whether the nonlinearity is a direct $\chi^{(5)}$ effect or a sequential $\chi^{(3)}:\chi^{(1)}$ effect is to study its dependence on laser pulsewidth. Results of our measurements are shown in Fig. 3c. When excited using 100 fs pulses (fluence: 1.04 J/cm^2 , intensity: $1.04 \times 10^{13} \text{ W/cm}^2$), pure toluene shows a strong limiting, which is not affected much by the addition of sample to it. On the other hand, when excited with 7 ns pulses (fluence: 7.47 J/cm^2 , intensity: $1.07 \times 10^9 \text{ W/cm}^2$) toluene shows only a weak nonlinearity, which increases significantly on the addition of nanoclusters. Thus the nonlinearity in toluene is instantaneous and intensity-dependent, whereas that in the nanoclusters is accumulative. An accumulative nonlinearity indicates the involvement of a sequential nonlinear process.

However, unlike in the case of semiconductors and metal colloids, the excitation dynamics in 29 kDa Au clusters should be modeled in a semi-molecular framework. This implies that the relative rigidity of the 140 atom cluster might impede the photogeneration of free carriers, but nevertheless, will not hinder the occurrence of an excited state absorption. At this point it is worthwhile to discuss the size-dependent transition of metal clusters from a ‘nanoparticle’ to ‘molecular’ type behavior. From studies in gold, Link et al. [21] have found strong evidence for the molecule-like behavior of a 28-atom gold core nanocluster surrounded by glutathione molecules. For instance, these clusters exhibit two sepa-

rate luminescence bands with maxima at 1.5 and 1.15 eV (800 and 1100 nm, respectively), and the luminescence lifetime is found to be in the order of nanoseconds to microseconds. Because of this unusually high lifetime, it was suggested that the short and long wavelength bands could be assigned to the fluorescence and phosphorescence from excited singlet and triplet states, respectively, in analogy to the photophysical properties of a molecule. Moreover, the excited state lifetimes were found to be independent of the pump intensity, revealing a single electron excitation dynamics typical of molecules. In comparison, in larger metal clusters (>2–3 nm) which show the ‘nanoparticle’ behavior, the prevalent plasmon excitation is a collective process, and the subsequent electron–phonon relaxation is strongly pump intensity dependent, due to the temperature dependence of the electronic heat capacity.

In the present case, however, the cluster contains about 140 atoms, and the SPR is extremely weak to the extent that no SPR bleach has been observed on laser excitation. Therefore the behavior is rather midway between that of a molecule and a nanoparticle, and hence, the term ‘semi-molecular’ may be an appropriate description. It is therefore possible to consider a four-level system for the electron dynamics of the clusters, as shown in Fig. 4. The one-photon excited level is not shown, since the linear transmission is normalized to unity in the calculations. In this scheme, two photons at 532 nm (2.33 eV) are required to reach the first non-linearly excited state, from where a fast decay occurs

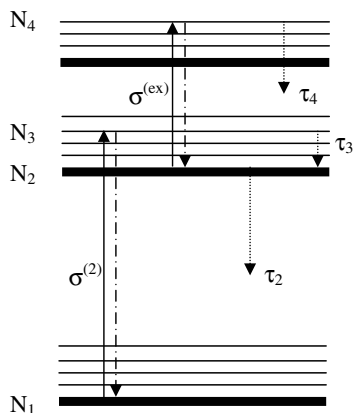


Fig. 4. A schematic energy level diagram for the Au clusters in the semi-molecular approximation. Downward transitions drawn close to the absorption transitions represent stimulated emission. Other decays are represented by their respective lifetimes, τ_n .

to the LUMO (lowest unoccupied molecular orbital) level. A third photon is hence absorbed, in an excited state absorption process. It may be noted that in a nanoparticle model for Au clusters, two-photon absorption at 2.33 eV will correspond to the interband transitions from the d-band to the conduction band, and excited state absorption will correspond to free carrier absorption. The LUMO state is relatively long-lived, and de-excitation occurs by radiative and non-radiative emissions bridging the HOMO (highest occupied molecular orbital) – LUMO gap. The corresponding set of rate equations can be written as:

$$\frac{dN_1}{dt} = -\frac{\sigma^{(2)}(N_1 - N_3)I^2}{2(h\nu)^2} + \frac{N_2}{\tau_2}, \quad (3)$$

$$\frac{dN_2}{dt} = -\frac{\sigma^{(ex)}(N_2 - N_4)I}{h\nu} - \frac{N_2}{\tau_2} + \frac{N_3}{\tau_3} + \frac{N_4}{\tau_4}, \quad (4)$$

$$\frac{dN_3}{dt} = \frac{\sigma^{(2)}(N_1 - N_3)I^2}{2(h\nu)^2} - \frac{N_3}{\tau_3}, \quad (5)$$

$$\frac{dN_4}{dt} = \frac{\sigma^{(ex)}(N_2 - N_4)I}{h\nu} - \frac{N_4}{\tau_4}, \quad (6)$$

and the propagation equation is,

$$\frac{dI}{dt} = \frac{-c}{n} \left\{ \frac{\sigma^{(2)}(N_1 - N_3)I^2}{h\nu} + \sigma^{(ex)}(N_2 - N_4)I \right\}, \quad (7)$$

where N_n are the populations of the respective levels, I is the intensity of the laser pulse, $\sigma^{(2)}$ is the two-photon absorption cross-section, and $\sigma^{(ex)}$ is the excited state absorption cross-section. τ_n are the lifetimes of the respective levels. Knowledge of τ_n is required to solve the above equations simultaneously for $\sigma^{(2)}$ and $\sigma^{(ex)}$ within reasonable limits of accuracy, and earlier studies have thrown some light into this aspect. For example, transient absorption studies in Au₂₈ have revealed that when excited at 400 nm, and probed at longer wavelengths (>500 nm), the excited state relaxation is a biexponential decay [21]. A subpicosecond (about 750 fs) lifetime and another longer (>1 ns) decay time are involved, independent of the laser pump power. The fast relaxation was attributed to the relaxation from the initially excited (Franck–Condon) state to the LUMO level. The longer decay time was assigned to the radiative and nonradiative recombinations taking place from the LUMO level, causing the final relaxation of the clusters.

To measure the excited state relaxation times of our samples, we did pump–probe studies using 100 fs,

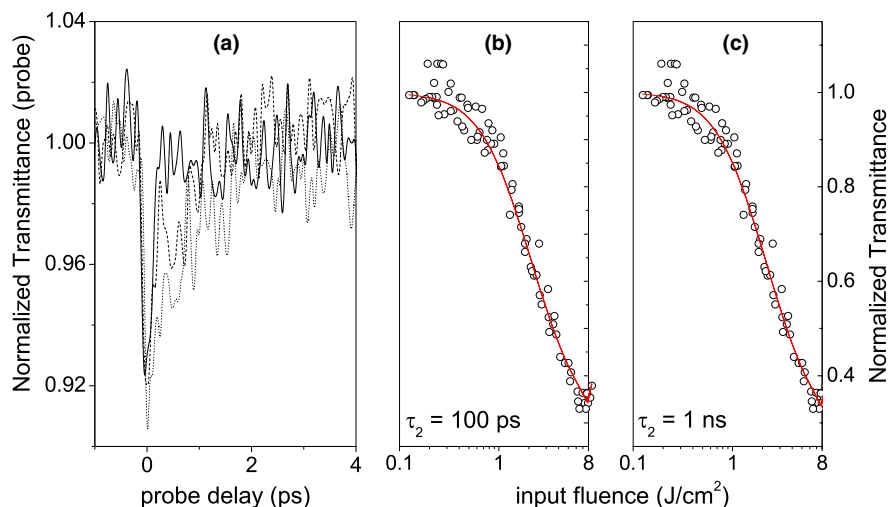


Fig. 5. (a) Transmission recovery of the Au₁₄₀ clusters when excited and probed with 400 nm, 100 fs pulses. Solid curve, pure toluene; dashed curve, hexanethiol protected cluster; dotted curve, dodecanethiol protected cluster. (b,c) Normalized transmittance of the Au@hexanethiol clusters with input laser fluence. Sample linear transmittance is 0.2. Solid curves are numerical fits obtained for two different values of τ_2 .

Table 1

Nonlinear absorption cross-sections calculated for Au@hexanethiol clusters under the nanoparticle and molecule approximations

Model	τ_2 (ps)	τ_3 (ps)	τ_4 (ps)	$\sigma^{(2)}$ (cm ⁴ s)	$\sigma^{(ex)}$ (cm ²)
Nanoparticle	100	1.4	0.6	5.89×10^{-45}	9×10^{-16}
Molecule	1000	1.4	0.6	6.82×10^{-46}	9×10^{-16}

400 nm pulses for pure toluene and the clusters. A weak fraction of the 400 nm pulse was used as the probe. Typical results are shown in Fig. 5a. Interestingly, we observe only the fast component of the decay, and the slow component is absent. This is consistent with the observation in Au₂₈ that when the probe wavelength is decreased, the amplitude of the slow component also decreases, since the transient absorption peak is redshifted to 600 nm (2.07 eV) [21].

From several pump–probe measurements we have estimated average values for the fast relaxation time, assuming a single exponential function. While pure toluene shows a lifetime of 501 ± 72 fs, hexanethiol protected 29 kDa clusters gives a lifetime of 1.17 ± 0.15 ps, and dodecanethiol protected 29 kDa gives 1.63 ± 0.17 ps. This lifetime should correspond to τ_3 in the energy level diagram. The radiative lifetime τ_2 (which is not measured) should be in the order of nanoseconds in a molecular model [21,22], and lesser in a nanoparticle model. Therefore, we have solved the rate equation system numerically under both approximations, to obtain the corresponding values of $\sigma^{(2)}$ and $\sigma^{(ex)}$. The values thus calculated are given in Table 1. These values are rather high, when compared to the typical absorption cross-sections in organic molecules. It is therefore evident that the nonlinear absorption in the present clusters is very strong.

5. Conclusions

Nanosecond laser excitation at 532 nm has revealed an accumulative nonlinearity in Au clusters in the size range of 29 kDa, containing about 140 atoms. The cluster properties are found to be semi-molecular, since they fall in between those of nanoparticles and molecular clusters. As the surface plasmon absorption band is almost absent in these clusters, plasmon bleach effects do not occur, and hence, the nonlinearity is exclusively of the optical limiting type. Induced thermal scattering is not prominent. Numerical fitting to the experimental data indicates that the limiting is caused by a two-photon induced excited state absorption process. The cross-sections calculated for two photon and excited state absorptions are rather high, in comparison to organic molecules. When excited at 400 nm the nonlinearity is very fast, with a lifetime of less than 2 ps. Because

of the above properties, these materials can be used as fast and efficient optical limiters at appropriate pump wavelengths.

Acknowledgements

T.P. acknowledges financial support from the Department of Science and Technology through the Nanoscience and Nanotechnology Initiative. Thanks are also due to the Department of Information Technology for supporting a research project on optical limiting of nanoparticles.

References

- [1] U. Kreibig, M. Vollmer, *Optical Properties of Metal Clusters*, Springer, Berlin, 1995.
- [2] E.J. Heilweil, R.M. Hochstrasser, *J. Chem. Phys.* 82 (1985) 4762.
- [3] S. Link, C. Burda, Z.L. Wang, M.A. El Sayed, *J. Chem. Phys.* 111 (1999) 1255.
- [4] J. Hohlfeld, S.-S. Wellershoff, J. Guedde, U. Conrad, V. Jaehnke, E. Matthias, *Chem. Phys.* 251 (2000) 237.
- [5] W. Eberhardt, *Surf. Sci.* 500 (2002) 242.
- [6] M. Anija, J. Thomas, N. Singh, A.S. Nair, T. Pradeep, R. Philip, *Chem. Phys. Lett.* 380 (2003) 223.
- [7] R. Philip, G.R. Kumar, N. Sandhyarani, T. Pradeep, *Phys. Rev. B.* 62 (2000) 13160.
- [8] F. Hache, D. Ricard, C. Flytzanis, U. Kreibig, *Appl. Phys. A* 47 (1988) 347.
- [9] M. Brust, M. Walker, D. Bethell, D.J. Schiffrin, R. Whyman, *J. Chem. Soc., Chem. Commun.* (1994) 801.
- [10] T.G. Schaaff, M.N. Shafiqullin, J.T. Khoury, I. Vezmar, R.L. Whetten, *J. Phys. Chem. B* 105 (2001) 8785.
- [11] J. Cyriac, V.R. Rajeevkumar, T. Pradeep, *Chem. Phys. Lett.* 390 (2004) 181.
- [12] M. Sheik-Bahae, A.A. Said, T.M. Wei, D.J. Hagan, E.W. Van Stryland, *IEEE J. Quant. Electron.* 26 (1990) 760.
- [13] S.R. Mishra, H.S. Rawat, S.C. Mehendale, K.C. Rustagi, A.K. Sood, R. Bandopadhyay, A. Govindaraj, C.N.R. Rao, *Chem. Phys. Lett.* 317 (2000) 510.
- [14] R.G. Ispasoiu, L. Balogh, O.P. Varnavski, D.A. Tomalia, T. Goodson Jr., *J. Am. Chem. Soc.* 122 (2000) 11005.
- [15] L. Francois, M. Mostafavi, J. Belloni, J.-F. Delouis, J. Delaire, P. Feneyrou, *J. Phys. Chem. B* 104 (2000) 6133.
- [16] R.L. Sutherland, *Handbook of Nonlinear Optics*, Marcel Dekker, New York, 1996.
- [17] A.A. Said, C. Wamsley, D.J. Hagan, E.W. Van Stryland, B.A. Reinhardt, P. Roderer, A.G. Dillard, *Chem. Phys. Lett.* 228 (1994) 646.
- [18] E.W. Van Stryland, H. Vanherzeele, M.A. Woodall, M.J. Soileau, A.L. Smirl, S. Guha, T.G. Boggess, *Opt. Eng.* 25 (1985) 613.
- [19] G.P. Banfi, V. Degiorgio, H.M. Tan, *J. Opt. Soc. Am. B* 12 (1995) 621.
- [20] P.V. Kamat, M. Flumiani, G.V. Hartland, *J. Phys. Chem. B* 102 (1998) 3123.
- [21] S. Link, M.A. El Sayed, T.G. Schaaff, R.L. Whetten, *Chem. Phys. Lett.* 356 (2002) 240.
- [22] B.A. Smith, J.Z. Zhang, U. Giebel, G. Schmid, *Chem. Phys. Lett.* 270 (1997) 139.